Journal of Molecular Catalysis B: Enzymatic 55 (2008) 130–136

Contents lists available at ScienceDirect

Journal of Molecular Catalysis B: Enzymatic

journal homepage: www.elsevier.com/locate/molcatb

Mutation of non-conserved amino acids surrounding catalytic site to shift pH optimum of *Bacillus circulans* xylanase

Seok Hwan Kim, Subarna Pokhrel, Young Je Yoo*

School of Chemical and Biological Engineering, Seoul National University, San 56-1, Shillim-dong, Gwanak-gu, Seoul 151-744, South Korea

ARTICLE INFO

Article history:
Received 19 July 2007
Received in revised form 15 February 2008
Accepted 26 February 2008
Available online 2 March 2008

Keywords:
Bacillus circulans xylanase
Optimum pH prediction
Non-conserved residues
Mutation

ABSTRACT

Improvement of enzyme function by engineering pH dependence of enzymatic activity is of importance for industrial application of *Bacillus circulans* xylanases. Target mutation sites were selected by structural alignment between *B. circulans* xylanase and other xylanases having different pH optima. We selected non-conserved mutant sites within 8 Å from the catalytic residues, to see whether these residues have some role in modulating pK_as of the catalytic residues. We hypothesized that the non-conserved residues which may not have any role in enzyme catalysis might perturb pK_as of the catalytic residues. Change in pK_a of a titratable group due to change in electrostatic potential of a mutation was calculated and the change in pH optimum was predicted from the change in pK_a of the catalytic residues. Our strategy is proved to be useful in selection of promising mutants to shift the pH optimum of the xylanases towards desired side.

1. Introduction

Bacillus circulans xylanase (BCX), low molecular weight endo-β-(1,4)-glycosidase family 11 (or G) xylanase, has emerged as a model xylanase with numerous potential applications in the food, pulp and paper industries. The major current application of xylanases is in the pulp and paper industries where the high temperature (55–70 °C) and alkaline pH of the pulp substrate requires thermo-alkalophilic enzymes for efficient bio-bleaching. Alkalophilic xylanases would also be required for detergent applications where high pHs are typically used. This family of xylanases (E.C.3.2.1.8) catalyzes the hydrolysis of main chain polysaccharide present in xylan, a main constituent of plant biomass, in an endowise manner yielding xylobiose and xylotriose [1,2]. Members of family 11 xylanases derive from both eukaryotic and bacterial species share sequence identity varying from 40 to 90% [3,4]. All members of this family show similar three-dimensional structures and active-site geometries but the pH optima vary widely from acidic values as low as 2 to alkaline values as high as 11 [4,5]. pH optimum is thus important for various industrial applications where the process runs in the pH range of 10–12, and hence any approach to shift pH optima of the xylanases towards alkaline range is desired.

BCX (20 kDa, 185 amino acid residues) catalyzes hydrolysis by double-displacement mechanism with retention of anomeric configuration (Fig. 1). At first, a covalent glycosyl-enzyme intermediate is formed and subsequently hydrolyzed via oxocarbanium-ion-like transition states. Two carboxylic acid residues suitably located in the active site are involved in the formation of the intermediate; one acts as a general acid catalyst (E172) by protonating the substrate, while the second performs a nucleophilic attack (E78) which results in the departure of the leaving group and the formation of the α-glycosyl enzyme intermediate (inversion of β to α-form). In the second step, the first carboxylate group now functions as a general base, abstracting a proton from a nucleophilic water molecule which attacks the anomeric carbon. This leads to a second substitution in which the anomeric carbon again passes via an oxocarbenium-ion-like transition state to give rise to a product with the β-configuration (inversion of α to β-form). Thus the overall result is retention of the configuration at the anomeric centre. These two glutamic acid residues are involved in an intricate network of hydrogen bonding contributed by highly conserved neighboring residues [4,6,7]. A better understanding of factors that establish the precise pK_a values of these catalytically essential groups will also aid in the engineering of enzymes with tailored pH optima. The pH-dependent activity of an enzyme is set primarily by the pK_a values of one or a few key ionizable groups within its active-site cleft [8]. The pK_a values of titratable groups in protein molecules are determined by the strength of the electrostatic field, and both the local hydrogen bonding network and solvent accessibility of

* Corresponding author. Tel.: +82 2 880 7411; fax: +82 2 887 1659.
E-mail address: yjyoo@snu.ac.kr (Y.J. Yoo).

1381-1177/$ – see front matter © 2008 Elsevier B.V. All rights reserved.
doi:10.1016/j.molcatb.2008.02.006

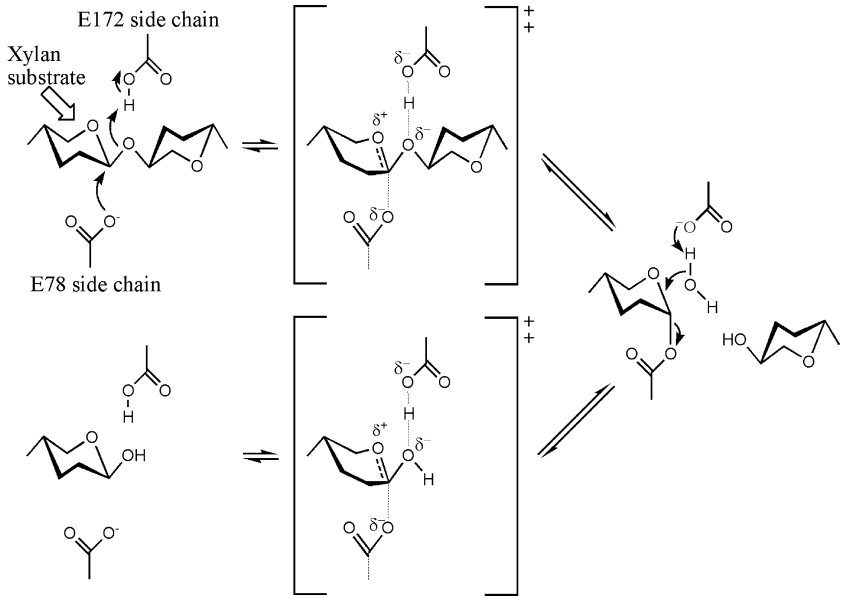

Fig. 1. General reaction mechanism for BCX (retaining glycosidases). Adapted from [7]. Figure was prepared with CS ChemDraw Ultra 8.0.

the titratable groups influence the electrostatic field. Electrostatic field, in the protein molecule, influences and correlates pK_a and the pH dependence of enzyme catalysis [9]. The pK_a values measured in experiments can thus yield useful information about the surrounding titratable groups, and can be measured directly using FT-IR [10] or by measuring the pH dependence of enzyme catalysis [11].

Torronen and Rouvinen [4] have partly clarified the basis of acidophilicity, and it appears that the pH profile is influenced by the nature of residues surrounding the catalytic residues whose pK_as are finely tuned by a complex hydrogen bond network. In the catalytic site of β-(1,4)-xylnases, an aspartic acid is hydrogen bonded to the acid/base catalyst whereas it is replaced by an asparagine in alkaline xylanases [5,12]. Furthermore, one report has shown a correlation between acidophilic adaptation and a decreased hydrophobicity around the two glutamic acid side chain involved in catalysis [13]. Moreover, site directed mutagenesis studies have shown the importance of neighboring residues in the fine tuning of pK_as of these catalytic site glutamate residues. Here, to further establish the role of non-conserved residues in determining pK_as, we have tried a series of mutations surrounding the catalytic site. It was hypothesized that the non-conserved residues might perturb pK_as of the catalytic residues and modulates pH optimum.

2. Experimental

2.1. Selection of target mutation sites

Seven family 11 xylanases were selected for structural alignment (Table 1). Homology modeling was carried out using *SWISS-MODEL* accessible via ExPaSy web server (http://expasy.org). *B. circulans* xylanase (pdb code: 1xnb) was adopted as a reference structure, and was aligned with the target xylanases using LOCK server (http://gene.stanford.edu/lock). The atomic coordinates of the target was generated using the reference structure. The non-conserved loops and missing side chains were rebuilt. Finally, optimization of bond geometry and relief of unfavorable non-bonded contacts was performed by 50 steps of steepest descent and by 500 steps of conjugate gradient energy minimization. The results from structural alignment were analyzed by DeepView/SwissPdb Viewer. A representation of Dayhoff's odds matrix [21] was used in selection of non-conserved mutation sites. In Dayhoff's odds matrix, amino acids that are close together are observed to be similar in physiochemical properties (size, hydrophobicity, etc.). Leucine (large non-polar) easily substitutes for valine (large non-polar) and such a change is said to be conserved. Glycine (small non-polar) does not easily substitute for arginine (large polar) and such a change is said to be non-conserved.

Table 1
Family G/11 xylanases

Microorganisms	pH optimum	Reference
Bacillus circulans	5.5	Esteban et al. [14]
Trichoderma ressei	5.3	Tenkanen et al. [15]
Thermomyces lanuginosus DSM 5826	7.0	Cesar and Mrsa [16]
Bacillus agaradhaerens	5.6	Nielsen et al. [17]
Clostridium stercorarium strain F9	7.0	Sakka et al. [18]
Streptomyces viridosporus T7A	7.0–8.0	Magnuson et al. [19]
Bacillus sp. Strain 41M-1	9.0	Nakamura et al. [20]

2.2. Mutant modeling and calculation of electrostatic potential

There are several published computational methods for electrostatic potential calculation to predict protein pK_a using the Poisson–Boltzmann equation. Delphi [22], GRASP [23] and UHBD [24] are well known tools used in many laboratories. Electrostatic potential was computed by *Delphi* of *InsightII* package, which obtains electrostatic energies from solutions to the Poisson–Boltzmann equation (Continuum model) [25]. The mutant modeling with single site mutation was carried out using BCX (pdb code: 1bvv, crystals prepared at pH 7.5) as the reference structure [26]. *Biopolymer* module of the *InsightII* was used to assign hydrogen and single site mutation to the structure. The energy of the mutation was then minimized using the *Discover* module of the *InsightII*. The environmental pH of both the wild and mutant enzyme models during the entire simulation process was kept 7.0, so as to homogenize the effect of pH on enzyme structure. *Delphi* was used to calculate electrostatic potential in and around enzyme molecule using a finite difference solution to the non-linear Poisson–Boltzmann equation. In *Delphi* (*InsightII*; *Delphi*, 2001), the potential is expressed in units of kT/e, and the change in pK_a is ΔpK_a. Since ΔpK_a equals to Δpotential/2.303, the difference in pH

optimum between wild type and mutant proteins (ΔpH optimum) can be predicted by calculating changes in electrostatic potentials of the catalytic residues. Generally, the dielectric constant in protein is expressed as a function of distance and is not same in all protein. The inner dielectric constant of the protein was set to 20 and the solvent was treated as a continuum with a dielectric constant of 80 and ionic strength of 0.05 M. The ion exclusion layer was set to 1.4 Å and grid size and grid points were set to 80 and 81, respectively.

Electrostatic potential and pK_a of a residue in protein are related with each other and the relation can be represented as shown in the following equation [27]:

$$\text{pH optimum} = \frac{pK_1 + pK_2}{2}, \quad \Delta\text{pH optimum} = \frac{\Delta pK_1 + \Delta pK_2}{2} = \frac{\Delta\Delta E_1 + \Delta\Delta E_2}{2 \times 2.303RT} = \frac{\Delta\text{Potential}_1 + \Delta\text{Potential}_2}{2 \times 2.303} \quad (1)$$

According to Eq. (1), pH optimum of enzyme is same as the average pK_as of catalytic residues and the electrostatic potential is linearly proportional to the pK_as of the residues.

2.3. Bacterial host strains, plasmids, media and culture conditions

Xylanase gene was amplified from *B. circulans*. *E. coli* DH5α and *E. coli* BL21 were used as cloning and expression hosts, respectively. *E. coli* DH5α was transformed by electroporation and plated on LB agar plate (100 μg/ml ampicillin) and grown at 37 °C for overnight. Single colony was transferred to 2 ml LB medium and grown at 37 °C for overnight.

2.4. Site directed mutagenesis

Site directed mutagenesis was performed using Pfu DNA polymerase according to the recommended protocol in QuickChange site directed mutagenesis kit (Stratagene). Primers used were: S84V (Sense): 5′-gattgaat attacgttgtcgacgtatggggaacgt accgtccg-3′, S84V (Antisense): 5′-cggacggtacgttccccatacgtcgacaac gtaatattcaatc-3′, A115I (Sense): 5′-caccaccac aagatacaacatacctttccatcgatgccga-3′, A115I (Antisense): 5′-tcgccatcgatggaaggtatgttgtatcttgtggtggtg-3′, A115S (Sense):5′-caccaccacaagatac aacagcccttccatcgatggcga-3′, A115S (Antisense): 5′-tcgccatcgatggaagggctgttgtatcttg tggtggtg-3′, A115T (Sense): 5′-ccaccacaagatacaacacaccttccatcgatggc-3′, A115T (Antisense): 5′-gccatcgatcg aaggtgtgttgtatcttgtggtgg-3′, A115W (Sense): 5′-caccaccacaagatacaactggccttccatcgatggcga-3′, A115W (Antisense): 5′-tcgccatcgatggaaggccagttgtatcttgtggtggtg-3′, A115Y (Sense): 5′-tacaccacc acaagatacaactacccttccatcgatggcga tc-3′, A115Y (Antisense): gatcgccatcgatggaagggtagttgtatcttgtgg tggtgta-3′. The polymerase chain reaction condition were 4 min at 95 °C; 16 times of 95 °C for 30 s, 55 °C for 1 min, 68 °C for 5 min. PCR products were purified and gel extracted and sent for DNA sequencing. DpnI endonuclease was used to select synthesized DNA with mutation. The synthesized DNA with mutation was transformed into *E. coli* DH5α by electroporation and plated on LB-agar plate containing ampicillin.

2.5. Protein expression and purification

Single colony from transformants was inoculated into 2 ml of LB medium (100 μg/ml ampicillin) and grown overnight. Four hundred microlitres of the culture was inoculated into 50 ml of fresh LB medium (100 μg/ml ampicillin) and grown at 37 °C with shaking until o.d. reaches 0.5–0.6. Induction was performed adding 1 mM of IPTG and was grown at 20 °C for 20 h. Cells were harvested by centrifugation and were suspended in 5 ml of lysis-buffer (50 mM NaH_2PO_4, 200 mM NaCl, 10 mM imidazole; pH 8.0). Cell debris was removed by centrifugation after disruption by sonication, and purification was done by affinity chromatography using Ni-chelate matrix (for His-protein) [28]. Protein was analyzed by SDS-PAGE [29].

2.6. Enzyme quantification and assay

Enzyme concentration was determined by modified Lowry method and assayed by dinitrosalicylic (DNS) acid method [30]. In DNS method, the xylanase activity is determined by measuring the release of oligosaccharides and reducing sugars. Colored product developed after the reaction of DNS with sugars is measured at 540 nm. The activity of xylanase as a function of pH was measured over a range of pH 4–9.

3. Results and discussion

The family 11 xylanases are single domain proteins composed of three anti-parallel β-sheets (14 β-strands) and one α-helix, with the active site lying between second and third sheet (Fig. 3). The active site of BCX is composed of several highly conserved residues arranged to form an intricate network of hydrogen bonds surrounding two catalytically essential glutamates (E78 and E172) which are ~6 Å apart. Similarly, two tyrosine residues Y69 and Y80, and R112 are shown to be involved in substrate binding, while a tryptophan is shown to participate either in stacking interaction or hydrogen bonding with the xylose ring of the substrate [6,31,32].

In the native enzyme structure of BCX, E78 is hydrogen bonded to Q127 and Y69, whereas E172 is hydrogen bonded to N35 and Y80. The pK_a values of E78 and E172, in the free BCX, were measured to be 4.6 and 6.7, respectively [33]. The increased pK_a value of 6.7 for E172, necessary for functioning as general-acid catalyst, appears to be due to electrostatic repulsion from the negatively charged E78. These values are in close agreement with those determined from the bell-shaped pH-activity profile of this enzyme and thereby provide a straightforward explanation for its observed pH optimum near 5.7 [33]. Hydrogen bonding network of the surrounding residues with acid/base catalyst is an important factor to modulate pK_a and thus to the pH optimum of the enzyme. Structural comparison of low molecular weight family 11 xylanases shows a strikingly common feature, in that the residue hydrogen bonded to the general acid/base catalyst is asparagine in so-called 'alkaline' xylanases, whereas it is aspartic acid in those with a more 'acidic' pH optimum [4]. Krengel and Dijkstra [31] proposed the possible mechanism of low pH optimum in *Aspergillus niger* xylanase. They hypothesized that the hydrogen bond between acid/base catalyst E170 and nearby D37 is stronger, and only at low pH, protonation of the aspartate residue might break this interaction, thereby making the proton available for xylan hydrolysis. In N35D mutant study of BCX, Joshi et al. [5] proposed 'reverse protonation' mechanism as the basis of low pH optimum. In their study, combination of NMR and kinetic studies demonstrated that the pH-dependent activity of N35D BCX is dictated by the ionization states of the nucleophile, E78, and the D35 and both the D35 and E172 act together as general acid/base catalyst. For alkaline xylanases, in which the aspartate residue is replaced by an asparagine, catalysis is then be possible at a much higher pH, since the asparagine side-chain can always serve not only as a hydrogen bond acceptor, but also as a hydrogen bond donor. Only at a pH high enough to deprotonate the acid–base catalyst would the upper pH limit be reached for these xylanases [31]. *Trichoderma reesei* xylanase (XYNII) is an alkaline xylanase with an asparagine residue at position 44 and a pH optimum of 5.3. In XYNII, N44 is involved in a weaker interaction (3.4–3.7 Å) with the acid/base catalyst E177 [12]. Though there are several reports explaining pK_a modulation of the xylanases, but it seems still a challenge to define experimentally and theoretically

Table 2
Structural alignment within 8 Å of the catalytic residues

B. circulans	*T. ressei*	*B. agaradhaerens*	*C. stercorarium* strain F-9	*Bacillus* sp. Strain 41M-1	*S. viridosporus* T7A	*T. lanuginosus* DSM 5826
W9			L			
Y26	F	F	F	F		
V28		A	C	A	T	T
W30						
T33	G	V	I	V	C	
G34		N		N		
N35		I	A	I	L	
F36		L	L	L		
V37						
V38	G	F	F	F	A	G
G39		R	R	R		
W58	Y	F	Y		F	Y
P60						
G62						
N63						
G64	S	A	S	S		S
Y65						
L66						
T67	S	C	C			A
L68	V	V	V	V		V
Y69						
G70						
W71						
T72	S					
R73		V		V	A	
P75						
L76						
I77		V	V	V	V	V
E78				F		
Y79						
Y80						
V82						
S84	N				N	N
W85	F					F
G86						
Y108						G
T110						
T111						
R112						
A115		Q		Q		
P116						
S117						
I118					V	
F125						
T126	Y	K	Q	Q	N	D
Q127						
Y128						
W129						
W153						
L160						
Y166						
M169	V	L	L	L		V
A170		T	T	T		
T171	V	V	V	V		
E172						
G173						
Y174						
Q175	F					F
S176						
S180	A	A	A	A		A

The vacant spaces in the table specify the same amino acid as in wild type.

the factors that establish the precise pK_a values of these catalytically essential groups along a given reaction pathway and thereby set the conditions of pH under which an enzyme is maximally active.

3.1. Selection of target mutation sites

Structural alignment of BCX and six other xylanases was performed to find out the properties of xylanases having higher pH optimum, and the xylanases having similar pH optimum to that of *B. circulans* and of other having higher pH optimum were selected for further analyses. If the range of structural alignment was set to 9–10 Å, all the residues were selected due to small size of xylanases. Therefore, we selected non-conserved sites within 8 Å from the catalytic residues, to see whether these residues have some role in modulating pK_as of the catalytic residues. The results of structural alignment are displayed in Table 2.

3.2. Mutant modeling and calculation of electrostatic potential

The differences in pH optimum between wild type and mutant proteins were predicted by calculating change in electrostatic

Table 3
Electrostatic potential and ΔpH optimum in wild type and mutants

	Wild type	R112N	Y80F	R73V	Q167M	Q127E	Q127A	N35D	N35A	Q175K
Glu 78										
OE1	−32.17	−30.87	−26.17	−32.93	−30.39	−38.27	−28.13	−34.31	−32.94	−32.28
OE2	−43.04	−36.17	−43.70	−39.98	−44.41	−46.92	−32.51	−44.65	−40.82	−42.95
Average potential	−37.6	−33.52	−34.93	−36.45	−37.4	−42.6	−30.32	−39.48	−36.88	−37.61
Glu 172										
OE1	−26.76	−28.51	−31.42	−27.1	−26.23	−29.1	−29.00	−28.95	−27.78	−26.82
OE2	−32.15	−33.41	−32.25	−31.91	−32.37	−34.22	−31.96	−34.22	−31.78	−32.12
Average potential	−29.45	−30.96	−31.83	−29.51	−29.3	−31.66	−30.48	−31.58	−29.78	−29.47
ΔpH optimum (Calculated)		+0.56	+0.06	+0.24	+0.08	−1.56	+1.36	−0.87	+0.09	−0.005
ΔpH optimum (Published reports)		+0.5	+0.6	+1.0	+2.0	−0.6	0	−1.0	0	0

potential of catalytic residues using *Delphi* module of *InsightII* which considers Poisson–Boltzmann equation. Initially, to check the utility of our computational method, nine mutations (N35D, N35A, R73V, Y80F, R112N, Q127A, Q127E, Q167M and Q175K) which had already published reports of their pH optima were considered for electrostatic potential computation (Table 3). Out of nine, calculated pH optima in four mutant models (R112N, N35D, N35A and Q175K) were almost same to their experimental values in published reports, where as the two mutant models (Q127A and Q167M) showed wide variation. The remaining three mutant models (Y80F, R73V and Q127E) showed somehow compromisable results. The accuracy of electrostatic potential calculation depends up on several factors like ionic strength, dielectric constant assigned to the protein interior, and even up on the computational artifacts which depend up on grid resolution and molecule mapping [22]. We have tried our best to optimize the parameters for the electrostatic potential calculation of the charged groups on catalytic glutamates in *B. circulans* xylanase. The wider deviation in calculated ΔpH optimum of Q127A and Q167M mutants could not be minimized with repeated trial, but at the same conditions, calculation on other six mutant models (Table 3) gave satisfactory result. Several pK_a calculation programs are poor at calculating the correct pK_a values for the catalytic residues which are often in extensive H-bonding network [34].

After getting encouraging results by the tool we followed, 10 non-conserved amino acid residues (V28, T33, F36, V38, G39, S84, A115, T126, T171 and Q175) were selected and each was substituted with 19 other amino acids, thus creating a library of 190 mutants. We considered single mutations to optimize computational method to shift the optimum pH of the xylanase towards desired side. The greater shift can be achieved by multiple-site mutations. Non-conserved residues were mutated because the conserved residues may have role in catalysis, folding, and conformational integrity of the enzyme. It was hypothesized that the non-conserved residues which may not have any role in enzyme catalysis might perturb pK_as of the catalytic residues. Among the pool of 190 mutant models, eighty mutant models showed upward shift in pH optima up on electrostatic potential computation (data not shown). Out of these eighty mutant models (single site mutation), six mutant models (S84V, A115S, A115I, A115T, A115Y and A115W) who showed maximum shift in pH optimum towards alkaline side were experimented in wet-lab for optimum pH and activity profiles (Table 4 and Fig. 2). Up on site directed mutagenesis experiment, five mutants (S84V, A115T, A115W, A115I and A115Y) showed change in pH optima towards alkaline side but the pH optimum of the mutant A115S was not changed rather it retained 95% of the original activity. Calculated change in pH optima of the mutants S84V and A115Y (+0.4337 and +0.4505 pH) were in close agreement to the experimental values (+0.5 pH unit in both), where as the mutant A115Y showed lower value of relative activity (53%) as

Table 4
Computational and experimental results

Mutants	pH optimum		Relative activity (%)
	Calculated	Experimental	
S84V	+0.4337	+0.5	95
A115S	+1.1563	0	95
A115I	+0.6249	+0.5	45
A115T	+0.2209	+0.5	83
A115Y	+0.4505	+0.5	53
A115W	+0.6578	+0.5	53

compared to that of the mutant S84V (95%). Mutants A115I and A115W (45 and 53% relative activity) had a slightly higher calculated change in pH optima (+0.6249 and +0.6578 pH) as compared to the experimental values (+0.5 pH unit in each).

We mutated A115 and S84. A115 lies in thumb region (Fig. 3) which is eight-residue long loop (A115, P116, S117, I118, D119, G120, D121 and R122) in BCX. The triad of residues that forms the tip of the thumb (P116, S117 and I118) and G120 are conserved in family 11 glycosyl hydrolases [35]. One study, in *T. reesei* xylanase, indicated that the thumb possesses an opening and closing capability that modifies both the topology and the binding capacity of the active site [36], and the precise position of the thumb determines the width of the catalytic cleft [37]. This movement is probably an intrinsic feature of GH-11 xylanases [36]. Position of the loop may be changed when a larger substrate binds in a slightly different conformation, which affects the distances from the nucleophile and acid/base catalyst to the substrate and thus to catalytic performance of the enzyme [6]. The thumb is connected to the main protein scaffold via β-strands B8 and B7, where A115 is located at the base of the thumb where as R122 delimits the thumb structure. So, the possible cause of decrease in relative activity in A115X

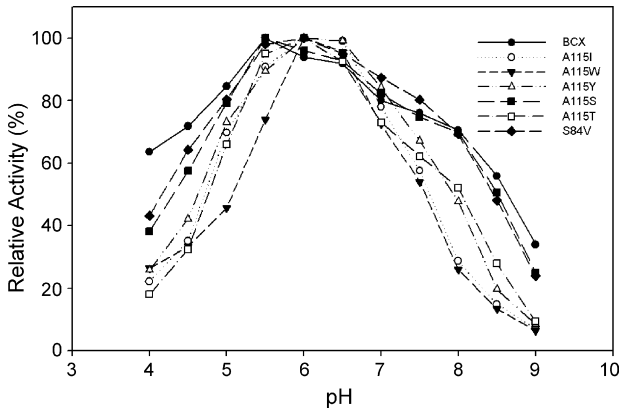

Fig. 2. Relative activities of the wild type BCX and mutants with respect to pH.

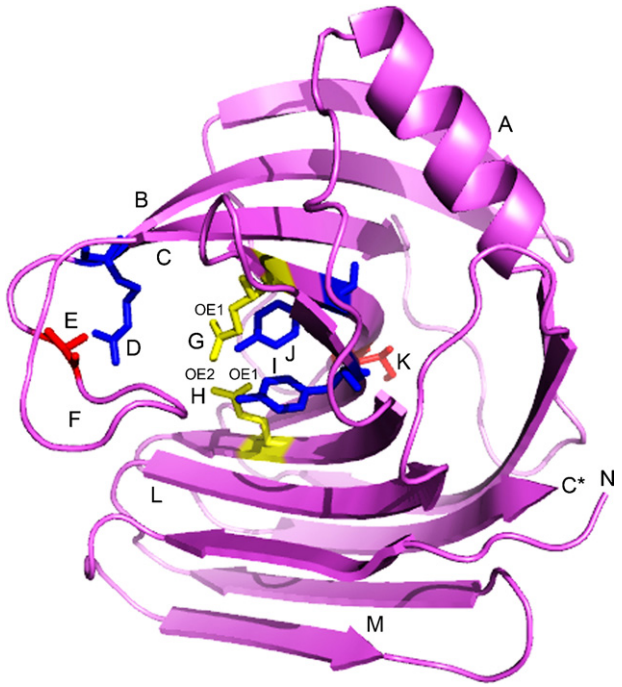

Fig. 3. Structure of BCX showing mutant sites Ala115 and Ser84, substrate binding residues (Tyr69, Tyr80 and Arg112) and catalytic residues (Glu78 and Glu172). A, α-helix; B, β-strand B8; C, β-strand B7; D, Arg112; E, Ala115; F, loop; G, Glu78; H, Glu172; I, Tyr69; J, Tyr80; K, Ser84; L, β-sheet B; M, β-sheet A; N, amino-terminal; C*, carboxy-terminal; OE1 and OE2, ε oxygen atom 1 and 2 in the catalytic glutamates (distance between Glu78 OE2/Glu172 OE2, 5.79 Å; distance between Glu78 OE2/Glu172 OE1, 5.57 Å; distance between Glu78 OE1/Glu172 OE2, 6.18 Å; distance between Glu78 OE1/Glu172 OE1, 5.97 Å).

mutants could be the disposition of the thumb or hindrance in proper movement of the thumb during substrate binding. The distance between A115 Cα/A115 Cβ and E78 Oε2 is 8.75 and 7.69 Å, respectively, where as the distance between A115 Cα/A115 Cβ and E172 Oε2 is 11.14 and 10.01 Å, respectively. Among the five A115X mutants, three mutations (A115I, A115Y and A115W) show hydrophobic property whereas the other two mutations (A115S and A115T) are hydrophilic in nature. Only the A115S mutant shows somewhat change in the hydrogen bonding interaction, but the other four mutants (A115I, A115T, A115Y and A115W) do not show any change in the hydrogen bonding interaction. S115 Oγ shows one extra hydrogen bond (3.18 Å) to Y113 O. Moreover, this only hydrogen bonding may not be the sole reason for no change in optimum pH of this mutant (A115S) as because Y113 does not show any change in hydrogen bonding network in A115S mutant model as compared to the wild type. So, the possible reason for increased optimum pH of the other three mutants (A115I, A115Y and A115W) could be due to increased hydrophobic interactions around the catalytic cleft as studied by using Protein Interactions Calculator [38]. A115 in wild type shows two hydrophobic interactions at 10 Å cut-off (with P116 and F125) where as A115I, A115Y and A115W shows four (with P116, F125, W129 and Y174), four (with P116, F125, W129 and Y174) and three (with P116, F125 and Y174) hydrophobic interactions at the same cut-off distance respectively. No change in optimum pH of the A115S can be due to weaker hydrophilic property of A115S mutation. Moreover, the change in Optimum pH of the A115T mutant remains unexplained as it does not show any change in hydrogen bonding and other interactions. S84 is located at a longer distance from both of the catalytic residues as compared to A115. The distance between S84 Cα/S84 Oγ and E78 Oε2 is 16.72 and 18.53 Å, respectively, where as the distance between S84 Cα/S84 Oγ and E172 Oε2 is relatively shorter (10.04 and 14.56 Å). On native structure studied (pdb code: 1bvv), S84 Oγ forms two H-bonds; one with L66 N (2.96 Å) and other is bonded with W58 Nε1 (3.05 Å). L66 is involved in extensive H-bonding network. S84 to V84 substitution breaks up the H-bonding network, which could play a possible role for shifting pH optimum of the mutant S84V towards alkaline side. S84V site is far apart from the catalytic residues, so, the substituted residue might not directly interact with the catalytic residues, but it is possible that the change in optimum pH of the mutants can be due to perturbation of the conserved and or non-conserved hydrogen bonding network which is seen around the nucleophile E78 and the acid/base catalyst E172.

4. Concluding remarks

We performed single site mutations of the two non-conserved residues (A115 and S84) in BCX. The decrease in relative activity in A115X mutants may be due disposition of the thumb or hindrance in proper movement of the thumb during substrate binding. The results of performing non-conservative mutations at the sites located far from the catalytic sites in BCX clearly show that such mutations play a significant role in modulation of pK_as of the catalytic residues and optimum pH of BCX. The strategy of performing non-conservative mutations and the parameters we optimized to calculate ΔpK_a of the catalytic glutamates in BCX using *Delphi* can be applied to select promising mutation sites to shift pH optima of the xylanases.

References

[1] B. Henrissat, A. Bairoch, Biochem. J. 316 (1996) 695–696.
[2] M.R. Bray, A.J. Clarke, Eur. J. Biochem. 204 (1992) 191–196.
[3] A. Torronen, C.P. Kubicek, B. Henrissat, FEBS Lett. 321 (1993) 135–139.
[4] A. Torronen, J. Rouvinen, J. Biotechnol. 57 (1) (1997) 137–149.
[5] M.D. Joshi, G. Sidhu, I. Pot, G.D. Brayer, S.G. Withers, L.P. McIntosh, J. Mol. Biol. 299 (2000) 255–279.
[6] W.W. Wakarchuk, R.L. Campbell, W.L. Sung, J. Davoodi, M. Yaguchi, Protein Sci. 3 (1994) 467–475.
[7] C.S. Rye, S.G. Withers, Curr. Opin. Chem. Biol. 4 (2000) 573–580.
[8] N.R. Gilkes, B. Henrissat, D.G. Kilburn, R.C. Miller Jr., R.A.J. Warren, Microbiol. Rev. 55 (1991) 303–315.
[9] S.E. Jackson, A.R. Fersht, Biochemistry 32 (1993) 13909–13916.
[10] J. Davoodi, W.W. Wakarchuk, R.L. Campbell, P.R. Carey, W.K. Surewicz, Eur. J. Biochem. 232 (1995) 839–843.
[11] D.M. Kiick, B.G. Harris, P.F. Cook, Biochemistry 25 (1986) 227–236.
[12] A. Torronen, J. Rouvinen, Biochemistry 34 (1995) 847–856.
[13] F. de Lemos Esteves, F. Ruelle, V. Lamotte-Brasseur, B. Quinting, J.M. Frere, Protein Sci. 13 (2004) 1209–1218.
[14] R. Esteban, J.R. Villanueva, T.G. Villa, Can. J. Microbiol. 28 (1982) 733–739.
[15] M. Tenkanen, J. Puls, K. Poutanen, Enzyme Microb. Technol. 14 (1992) 566–574.
[16] T. Cesar, V. Mrsa, Enzyme Microb. Technol. 19 (1996) 289–296.
[17] P. Nielsen, D. Fritze, F.G. Priest, Microbiology 141 (1995) 1745–1761.
[18] K. Sakka, K. Yoshikawa, Y. Kojima, S. Karita, K. Ohmiya, K. Shimada, Biosci. Biotechnol. Biochem. 57 (1993) 268–272.
[19] T.S. Magnuson, M.A. Roberts, D.L. Crawford, G. Hertel, Appl. Biochem. Biotechnol. 28 (1991) 433–443.
[20] S. Nakamura, R. Nakai, K. Namba, T. Kubo, K. Wakabayashi, R. Aono, K. Horikoshi, Nucleic Acids Symp. Ser. (1995) 99–100.
[21] W.R. Taylor, J. Theor. Biol. 119 (1986) 205–218.
[22] I. Klapper, R. Hagstrom, R. Fine, K. Sharp, B. Honig, Proteins 1 (1986) 47–59.
[23] A. Nicholls, K. Sharp, B. Honig, Proteins 11 (1991) 281–296.
[24] J.D. Madura, J.M. Briggs, R.C. Wade, M.E. Davis, B.A. Luty, A. Ilin, J. Antosiewicz, M.K. Gilson, B. Bagheri, L.R. Scott, J.A. McCammon, Comput. Phys. Commun. 91 (1995) 57–95.
[25] Y.Y. Sham, Z.T. Chu, A. Warshel, J. Phys. Chem. 101 (1997) 4458–4472.
[26] G. Sidhu, S.G. Withers, N.T. Nguyen, L.P. McIntosh, L. Ziser, G.D. Brayer, Biochemistry 38 (17) (1999) 5346–5354.
[27] M.D. Joshi, G. Sidhu, J.E. Nielsen, G.D. Brayer, S.G. Withers, L.P. McIntosh, Biochemistry 40 (2001) 10115–10139.
[28] Z.L. Li, M.B. Terry, B. Robert, Biochem. Biophys. Acta 1460 (2000) 384–389.
[29] U.K. Laemmli, Nature 227 (1970) 680–685.
[30] G.L. Miller, Anal. Chem. 31 (1959) 426–428.
[31] U.B. Krengel, W. Dijkstra, J. Mol. Biol. 263 (1996) 70–78.

[32] H. Balakrishnan, L. Satyanarayana, S.M. Gaikwad, C.G. Suresh, Enzyme Microb. Technol. 39 (2006) 67–73.
[33] L.P. McIntosh, G. Hand, P.E. Johnson, M.D. Joshi, M. Korner, L.A. Plesniak, L. Ziser, W.W. Wakarchuck, S.G. Withers, Biochemistry 35 (1996) 9958–9966.
[34] J.E. Nielsen, G. Vriend, Proteins: Struct. Funct. Genet. 43 (2001) 403–412.
[35] A. Sapag, J. Wouters, C. Lambert, P. de Ioannes, J. Eyzaguirre, E. Depiereux, J. Biotechnol. 95 (2) (2002) 109–131.
[36] J. Muilu, A. Torronen, M. Perakyla, J. Rouvinen, Proteins 31 (1998) 434–444.
[37] R.L. Campbell, D.R. Rose, W.W. Wakarchuk, R. To, W.S. Sung, M. Yaguchi, in: P. Suominen, T. Reinikainen (Eds.), *Trichoderma reesei* Cellulases and Other Hydrolases, vol. 8, Foundation for Biotechnical and Industrial Fermentation Research, Espoo, Finland, 1993, pp. 63–72.
[38] K.G. Tina, R. Bhadra, N. Srinivasan, Nucleic Acids Res. 35 (2007) W473–W476.